JC124 confers multimodal neuroprotection in epilepsy by suppressing NLRP3 inflammasome activation: evidence from animal and human neuronal models

1. Supplementary materials and methods

1.1 Summary-based Mendelian Randomization (SMR) analysis

This GWAS dataset explicitly categorizes epilepsy types into three groups: focal epilepsy (FE), genetic generalized epilepsy (GGE), and unclassified epilepsy, with GGE further subdivided into four subtypes: juvenile myoclonic epilepsy (JME), childhood absence epilepsy (CAE), juvenile absence epilepsy (JAE), and generalized tonic-clonic seizures alone (GTCSA).

Supplementary Table 1. Information on the summary data from expression quantitative trait loci study and genome-wide association study

Summary data	Resource	Sample size and population ancestry
Expression quantitative trait loci (eQTL) for *NLRP3*	eQTLGen Consortium [1]	31,684 predominantly European
Epilepsy	International League Against Epilepsy Consortium on Complex Epilepsies [2]	52,538 controls and 29,944 people with epilepsy. The cases of epilepsy are predominantly of European descent (92%), with smaller proportions of African (3%) and Asian (5%) ancestry

1.2 Genotyping of *NLRP3* knockout (*NLRP3*$^{-/-}$) mice and *NLRP3* wild-type (*NLRP3*^{WT}) mice

In accordance with the instructions of the genotyping kit (YK-MG-100, UBIGENE,

Guangzhou, China), 1.5 mm mouse tails were clipped and placed in 2 mL EP tubes with 100 μL of tail lysis, and the EP tubes were placed in a metal bath at 95°C and incubated for 20 minutes. The following polymerase chain reaction (PCR) system was prepared in a 96-well PCR plate: 12.5 μL of Direct PCR Taq mix, 1 μL of mouse tail lysis product, 2 μL of identification primers and 9.5 μL of ddH_2O. After PCR amplification, nucleic acid electrophoresis was carried out on a 1.5% agarose gel (Biowest, Spain), 5 μL of the samples to be tested or a DNA ladder (Solarbio, Beijing, China) was added to each well, and electrophoresis was carried out at a constant voltage of 150 V for 40 minutes. Finally, a fusion imaging system (Fusion Imaging, UT, USA) was used to observe the DNA bands in the gel and determine the genotype of the mice.

1.3 Kainic acid (KA)-induced acute seizure mouse model and JC124 treatment

To identify the optimal dose of JC124 for inhibiting seizures in a KA-induced acute seizure mouse model, different doses of JC124 (0, 16.7, 50, 100, and 150 mg/kg) were used in preliminary experiments [3, 4]. Fifty wild-type male C57BL/6J mice, aged 7 to 8 weeks and weighing 22-25 g, were randomly divided into five groups. The mice were anesthetized with pentobarbital (50 mg/kg, intraperitoneal injection). A nickel–chromium alloy electrode (Plexon, HK) and a cannula (RWD, Shenzhen, China) were inserted into the Cornus Ammonis (CA) 1 region of the right hippocampus [millimeters (mm) from the bregma, anteroposterior, -2.0 mm; mediolateral, -1.5 mm; dorsoventral, -1.5 mm] and then fixed with bone cement. All the mice were allowed a seven-day postoperative recovery period before JC124 administration. Mice received different doses of JC124 intraperitoneally once a day for 7 consecutive days. After the 7th administration of JC124, 10 ng/0.5 μL of KA (Sigma–Aldrich, MO, USA) was administered via a cannula into the CA1 region of the right hippocampus to induce seizures [5, 6]. Seizure grades were estimated using Racine′s scale, the latency to the first seizure, the number and duration of seizures in grade 0-3 and grade 4-5 within 3 hours were recorded [5-7]. The behavioral and electrophysiological data were evaluated by two trained researchers, who were blinded to the experimental

conditions.

1.4 Measurement of hippocampal local field potential (LFP)

The mice were anesthetized with pentobarbital (50 mg/kg, intraperitoneal injection). For hippocampal LFP measurement, a nickel–chromium alloy electrode (Plexon, HK) was inserted into the CA1 region of the right hippocampus (coordinates as before) after KA injection and then fixed with bone cement. After 4 weeks of JC124 administration, the hippocampal LFP was recorded using an MAP data acquisition system (Plexon). The signals were filtered (0.1 to 500 Hz), preamplified (1000×), and digitized at 4 kHz. The number of seizure-like events (SLEs), the mean duration of SLE and the cumulative duration of SLEs were analyzed using NeuroExplorer software (Nex Technologies, MA, USA) [8-10]. SLE was defined as a cluster of spontaneous paroxysmal discharges with a frequency greater than 1 Hz and high-amplitude spike activity that was twice as great as the baseline, lasting more than five seconds [8, 11]. The behavioral and electrophysiological data were evaluated by two trained researchers, who were blinded to the experimental conditions.

1.5 Differentiation of human induced pluripotent stem cell (hiPSC)-derived neurons

hiPSCs were differentiated into neurons according to our previously reported methods [12]. High-quality hiPSCs (DYR0100) were manually selected for subsequent experimentation, and cell pluripotency was identified by immunofluorescence staining with anti-OcT4 and anti-SSEA4 antibodies.

hiPSCs that reached a confluence of 80% or more were chosen to initiate ectodermal differentiation. After a continuous induction period of seven days, the culture medium was switched to neural stem cell (NSC) medium (A1647801, Gibco, NY, USA). Culturing continued for an additional seven days until signs of spontaneous differentiation were observed. The cells were then transferred to 96-well culture plates with low adhesion for suspension culture. Ectoderm verification was performed through immunofluorescence staining with anti-PAX6 and anti-Nestin

antibodies.

The round spheres of NSCs were separated using accutase cell detachment solution (#07920, STEMCELL) and inoculated into culture plates coated with laminin (L6274, Sigma-Aldrich, MO, USA) and poly-D-lysine (27964-99-4, Sigma-Aldrich). The progression from NSCs to neurons was meticulously monitored. Furthermore, it is essential that BrainPhys neuronal medium (#05790, STEMCELL) be administered gradually, allowing neurons to undergo further maturation in vitro for a period of up to 60 days. Identification of neurons was conducted using immunofluorescence staining with an anti-MAP2 antibody.

1.6 Western blotting

Total protein was extracted from the hippocampus with a total protein extraction kit (BC3710, Solarbio, Beijing, China), and the protein concentration was determined with an enhanced bicinchoninic acid (BCA) assay kit (Beyotime, Shanghai, China). Each electrophoresis lane was loaded with 30 μg of protein, and the proteins were separated via electrophoresis using a 10% or 12% sodium dodecyl sulfate–polyacrylamide gel (SDS–PAGE, Beyotime, China). Proteins were then transferred to a polyvinylidene fluoride (PVDF) membrane (Millipore, MA, USA). After being blocked with 5% nonfat milk in Tris-buffered saline with 0.1% Tween 20 (TBST), the PVDF membranes were incubated overnight at 4°C with the following primary antibodies: anti-NLRP3 (1:1500, #15101, Cell Signaling Technology (CST), MA, USA), anti-ASC (1:1200, #67824, CST), anti-Caspase-1 (1:1200, #3866, CST), anti-Caspase-1 p10 (1:1200, AF4022, Affinity, OH, USA), anti-GSDMD (1:800, 20770-1-AP, Proteintech, Wuhan, China), and anti-GAPDH (1:10000, 60004-1-Ig, Proteintech). The PVDF membranes were washed with TBST 3 times for 5 minutes each time after primary antibody incubation and then incubated with horseradish peroxidase (HRP)-conjugated goat anti-mouse or anti-rabbit IgG (H+L) secondary antibodies (1:4000, SA00001-1, SA00001-2, Proteintech) at room temperature for 1 hour. After being washed with TBST, the PVDF membranes were incubated with an enhanced chemiluminescence (ECL) substrate (Affinity) and visualized on a fusion

imaging system (Fusion Imaging). The primary and secondary antibodies on the PVDF membrane were fully removed by stripping buffer (Beyotime), and then the PVDF membrane was incubated with another primary antibody. The intensity of each band was quantified with ImageJ 1.8.0 software (National Institutes of Health, MD, USA), and the GAPDH level was used as an internal loading control.

1.7 Immunohistochemistry

Paraffin sections were deparaffinized in xylene and then rehydrated by serial immersion in 100%, 95%, 80%, and 75% ethanol and phosphate-buffered saline (PBS). After antigen retrieval, the brain sections were treated with 3% H_2O_2 at room temperature for 10 minutes and blocked with 5% bovine serum albumin (BSA) at 37°C for 30 minutes. Then, the brain sections were incubated with primary antibodies: anti-NLRP3 (1:150, bs-10021R, BIOSS, Beijing, China), anti-ASC (1:200, #67824, CST), anti-Caspase-1 p10 (1:150, AF4022, Affinity), anti-GSDMD (1:150, 20770-1-AP, Proteintech), anti-IL-1β (1:150, 26048-1-AP, Proteintech), anti-IL-18 (1:150, 10663-1-AP, Proteintech), anti-Nrf2 (1:150, bs-1074R, BIOSS) and anti-HO-1 (1:150, bs-2075R, BIOSS) at 4°C overnight. After washing with PBS, the brain sections were incubated with HRP-conjugated anti-rabbit IgG (BOSTER, Wuhan, China) at 37°C for 35 minutes and then visualized with diaminobenzidine (DAB, BOSTER). Next, the sections were counterstained with hematoxylin, dehydrated, and mounted with neutral resins (BOSTER). Finally, images of the CA1 regions of the hippocampus were taken (OLYMPUS, Tokyo, Japan), and the mean optical densities (OD) of the immunohistochemical images were quantified using Image-Pro Plus 6.0 software (Media Cybernetics, ME, USA).

1.8 Immunofluorescence staining

After antigen retrieval and permeabilization, the brain sections were washed with PBS 3 times for 5 minutes each and then blocked with 5% normal goat serum (Solarbio) in PBS at 37°C for 1 hour, followed by the addition of antibodies: anti-NLRP3 (1:150, bs-10021R, BIOSS), anti-ASC (1:400, #67824, CST), anti-Caspase-1 p10 (1:150,

AF4022, Affinity), anti-GSDMD (1:150, 20770-1-AP, Proteintech), anti-GFAP (1:800, sc-33673, Santa Cruz, CA, USA), anti-Iba1 (1:350, GT10312, GeneTex, CA, USA), and anti-NeuN (1:450, MAB377, Millipore, MA, USA) at 4°C overnight. The brain sections were subsequently treated with the following species-specific secondary antibodies and incubated at 37°C for 1 hour: coraLite488-conjugated goat anti-rabbit IgG(H+L) (1:500, SA00013-2, Proteintech) and coraLite594-conjugated goat anti-mouse IgG(H+L) (1:500, SA00013-3, Proteintech). The brain sections were mounted with mounting medium containing DAPI (Southern Biotech, AL, USA), and fluorescence images of the CA1 regions of the hippocampus were taken with a confocal microscope (Nikon, A1R HD25, NY, USA). The numbers of microglia and astrocytes were analyzed with ImageJ 1.8.0 software. The data were expressed as the mean number of cells per square millimeter.

During the differentiation of hiPSC-derived neurons, cells at different stages of differentiation were stained using immunofluorescence. Cells were fixed with 4% paraformaldehyde for 30 minutes at 37 °C and then washed three times with PBS for 5 minutes each. This was followed by permeabilization with 0.1% Triton X-100 for 30 minutes and blocking with goat serum for 1 hour at 37 °C. The cells were incubated overnight at 4 °C with the following primary antibodies: anti-OcT4 (1:100, 381335, ZENBIO, Chengdu, China), anti-SSEA4 (1:100, ab16287, Abcam, Cambridge, UK), anti-PAX6 (1:200, 67529-1-Ig, Proteintech), anti-Nestin (1:100, R381211, ZENBIO) and anti-MAP2 (1:200, 250035, ZENBIO). The next day, cell slides were washed with PBS, followed by the addition of the corresponding fluorescent secondary antibody, and incubated for 1 hour at 37 °C in the dark. After sealing the slides, cells were observed under a fluorescence microscope and photographed (Nikon, A1R HD25).

1.9 Hematoxylin–eosin (HE) staining

Paraffin sections were deparaffinized in xylene and then rehydrated by serial immersion in 100%, 95%, 80% and 75% ethanol and water. The sections were placed in hematoxylin staining solution (G1076, Servicebio, Wuhan, China) for 3 minutes,

rinsed under running water for 3 minutes, placed in differentiation solution (G1076, Servicebio) for 3 seconds, rinsed under running water for 3 minutes, placed in hematoxylin bluing solution (G1076, Servicebio) for 1 minute, and rinsed under running water for 3 minutes. The sections were subsequently dehydrated in 95% ethanol for 1 minute and then placed in eosin staining solution (G1076, Servicebio) for 20 seconds. Finally, the sections were dehydrated, mounted with neutral resins (BOSTER) and observed under a microscope (OLYMPUS).

1.10 Molecular dynamics (MD) simulation

The starting configuration for the simulations involved protein complexes embedded within a cubic water box (the buffer distance was set at 10 Å). Physiological relevance was achieved using the SPC water model in combination with a 0.15 M NaCl solution. The systems were minimized and equilibrated after solvation to achieve optimal accuracy and stability in the simulations. Subsequently, 300 nanoseconds (ns) MD simulations were employed using Maestro 13.5 software (Schrödinger, NY, USA) under conditions of a pressure of 1 atm and a temperature of 300 K [13].

1.11 Statistical analysis

All data are presented as means ± S.E.M. Statistical analyses were performed using SPSS Statistics 29.0 and Graphpad Prism 10.0. The normality of the data was assessed using the Shapiro–Wilk test. Data from Figures 1, 2A, 2F-H, 3, 4, 5, 6 and 12, as well as Supplementary Figures 1, 3, 5C-D and 6, were subjected to one-way ANOVA followed by Tukey′s post hoc test. The statistical analyses for Figures 7, 8A, 8F-H, 9 and 10, as well as Supplementary Figures 4, 5E-F and 7, utilized two-way ANOVA with Tukey′s post hoc test. Finally, the data in Figures 2C-D, 8C-D and Supplementary Figure 8A were evaluated using repeated-measures ANOVA with Tukey′s post hoc test. All tests were two-sided, with statistical significance set at $p < 0.05$. Data were analyzed by two trained researchers, who were blinded to the experimental grouping. In the figures, each 'n' corresponds to either an individual

animal or a separate sample.

2. Supplementary results

2.1 Effects of different doses of JC124 on acute seizures

Compared with the 16.7 mg/kg dose group of JC124, the 50 mg/kg group significantly inhibited seizures in a KA-induced acute seizure mouse model. There were no significant differences in the latency to the first seizure and the number and total duration of seizures of grade 0-3 and grade 4-5 between the 50 and 100 mg/kg groups (Supplementary Fig. 1B-F). Additionally, higher doses of JC124 (100 mg/kg and 150 mg/kg groups) caused listlessness and weight loss in the mice. Therefore, 50 mg/kg of JC124 was selected for the subsequent experiments and for studying the involved mechanisms.

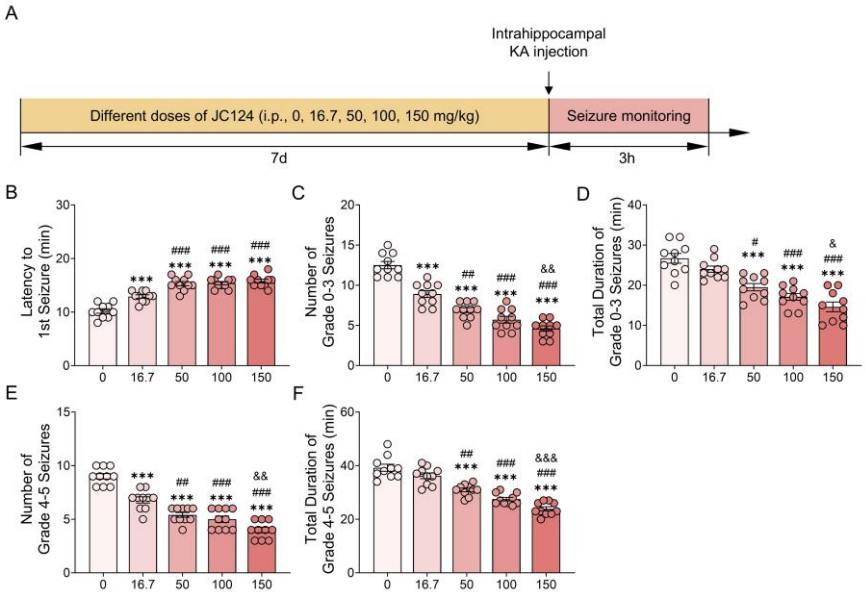

Supplementary Fig. 1 Effects of different doses of JC124 on acute seizures

(A) Study design timeline. (B) The latency to the first seizure, (C) the number of grade 0-3 seizures, (D) the total duration of grade 0-3 seizures, (E) the number of grade 4-5 seizures, and (F) the total duration of grade 4-5 seizures. n = 10. Data are presented as mean ± S.E.M. ***$p < 0.001$ versus the 0 mg/kg group. $^{\#}p < 0.05$, $^{\#\#}p < 0.01$, $^{\#\#\#}p < 0.001$ versus the 16.7 mg/kg group. $^{\&}p < 0.05$, $^{\&\&}p < 0.01$, $^{\&\&\&}p < 0.001$ versus the 50 mg/kg group.

2.2 Genotyping of *NLRP3*^{WT}, *NLRP3*$^{+/-}$ and *NLRP3*$^{-/-}$ mice

Electrophoretic bands of *NLRP3* gene expression in wild-type mice (*NLRP3*^{WT}, 666 bp only; mice 1, 3, 4, 6 and 8), *NLRP3* heterozygous knockout mice (*NLRP3*$^{+/-}$, 666 and 850 bp; mice 2, 5, 7, 9, 10 and 11) and *NLRP3* homozygous knockout mice (*NLRP3*$^{-/-}$, 850 bp only; mice 12, Supplementary Fig. 2).

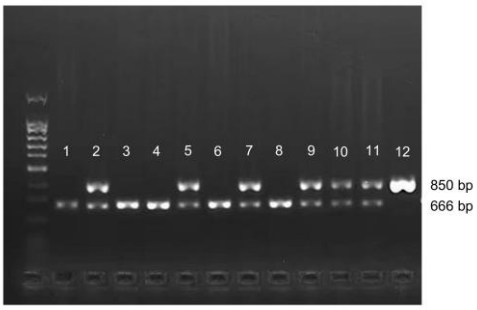

Supplementary Fig. 2 Genotyping of *NLRP3*^{WT}, *NLRP3*$^{+/-}$ and *NLRP3*$^{-/-}$ mice

Electrophoretic bands of *NLRP3* gene expression in *NLRP3*^{WT}, *NLRP3*$^{+/-}$ and *NLRP3*$^{-/-}$ mice.

2.3 Effect of JC124 treatment on status epilepticus (SE) in KA-treated mice

No significant differences were observed in the latency to the first occurrence of seizure (grade 0-2, 3, 4, and 5 seizures), latency to the onset of SE, and duration of SE between the groups (Supplementary Figs. 3 and 4).

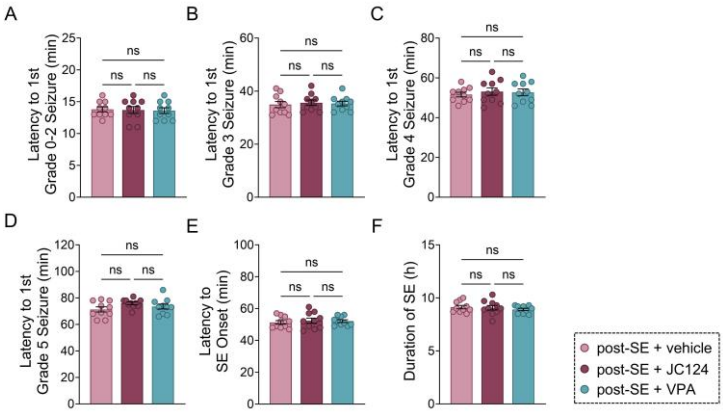

Supplementary Fig. 3 Effect of JC124 or valproic acid (VPA) treatment on SE in KA-treated mice

(A) Latency to the first grade 0-2 seizure, (B) latency to the first grade 3 seizure, (C) latency to the first grade 4 seizure, (D) latency to the first grade 5 seizure, (E) latency

to SE onset, and (F) duration of SE. *n* = 10. Data are presented as mean ± S.E.M. ns, not statistically significant.

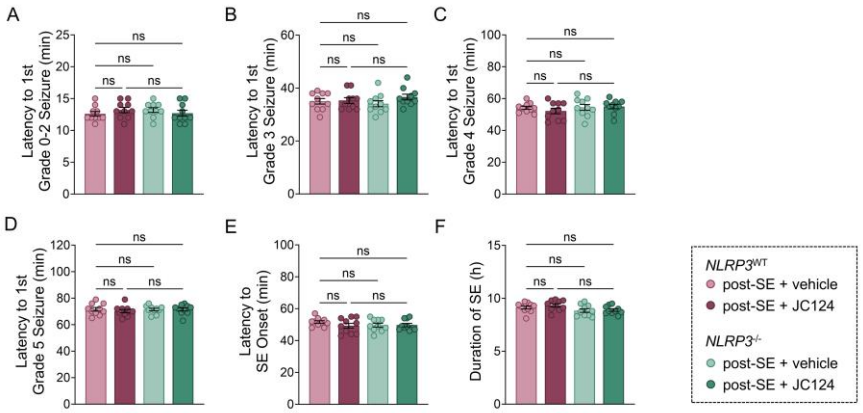

Supplementary Fig. 4 Effect of JC124 treatment on SE in KA-treated *NLRP3*^{WT} and *NLRP3*$^{-/-}$ mice

(A) Latency to the first grade 0-2 seizure, (B) latency to the first grade 3 seizure, (C) latency to the first grade 4 seizure, (D) latency to the first grade 5 seizure, (E) latency to SE onset, and (F) duration of SE. *n* = 10. Data are presented as mean ± S.E.M. ns, not statistically significant.

2.4 Effect of JC124 treatment on nonconvulsive spontaneous recurrent seizure (SRS) in KA-induced epileptic mice

Compared with those in the post-SE + vehicle group, 4-week continuous treatment with JC124 or VPA significantly prolonged the latency to the first nonconvulsive SRS and reduced the number of nonconvulsive SRSs (Additional file 1: Supplementary Fig. 5C-D).

This study revealed that JC124 administration significantly prolonged the latency to the first nonconvulsive SRS and reduced the number of nonconvulsive SRSs in KA-treated *NLRP3*^{WT} mice. However, this effect was not significant following the administration of JC124 to KA-treated *NLRP3*$^{-/-}$ mice (Additional file 1: Supplementary Fig. 5E-F).

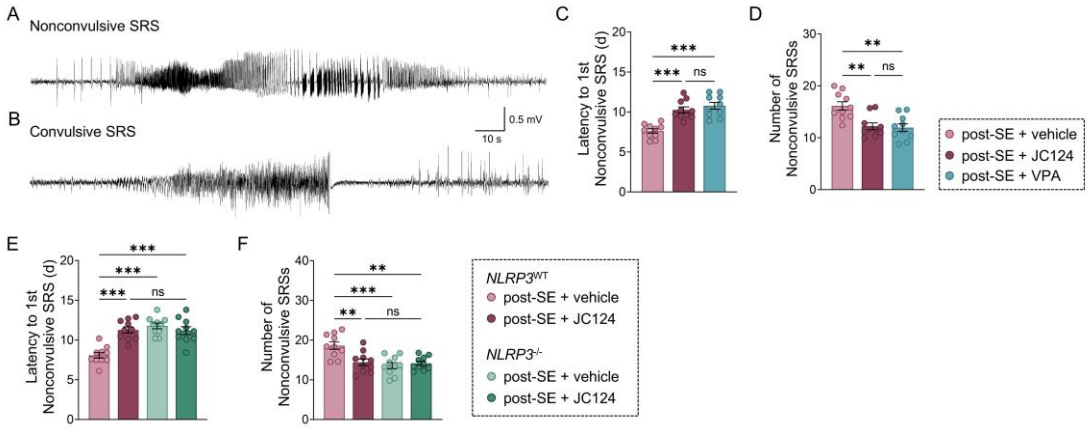

Supplementary Fig. 5 Effect of JC124 treatment on nonconvulsive SRS in KA-induced epileptic mice

Representative images of (A) the first nonconvulsive SRS and (B) the first convulsive SRS. (C) Latency to the first nonconvulsive SRS and (D) number of nonconvulsive SRSs in the post-SE + vehicle, post-SE + JC124, and post-SE + VPA groups. (E) Latency to the first nonconvulsive SRS and (F) number of nonconvulsive SRSs in the *NLRP3*^{WT} + post-SE + vehicle, *NLRP3*^{WT} + post-SE + JC124, *NLRP3*$^{-/-}$ + post-SE + vehicle, and *NLRP3*$^{-/-}$ + post-SE + JC124 groups. $n = 10$. Data are presented as mean ± S.E.M. *$p < 0.05$, **$p < 0.01$, ***$p < 0.001$. ns, not statistically significant.

2.5 Effect of JC124 treatment on locomotor ability in mice

In the open field test (OFT), no significant differences in movement time or distance were found among the groups (Supplementary Figs. 6 and 7).

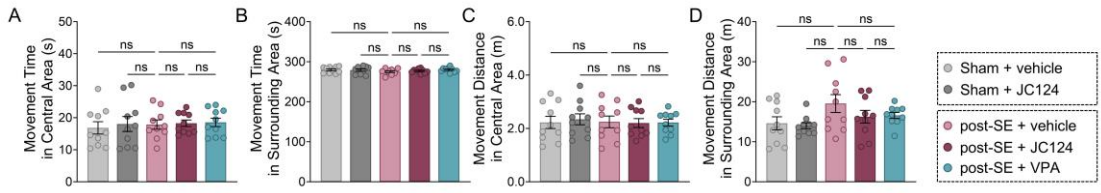

Supplementary Fig. 6 Effect of JC124 or VPA treatment on locomotor ability in KA-induced epileptic mice

(A) The movement time in the central area, (B) the movement time in the surrounding area, (C) the movement distance in the central area, and (D) the movement distance in the surrounding area. $n = 10$. Data are presented as mean ± S.E.M. ns, not statistically

significant.

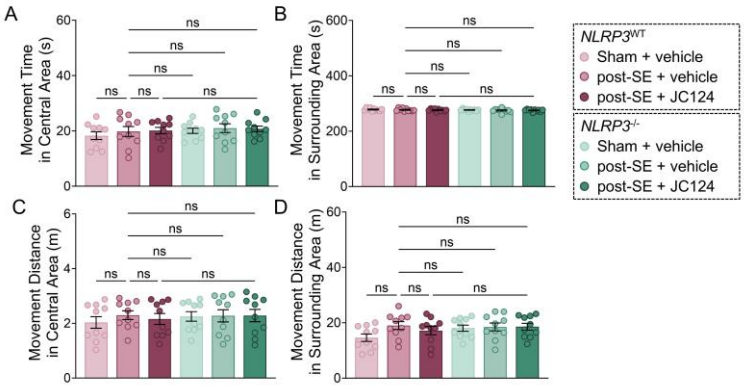

Supplementary Fig. 7 Effect of JC124 treatment on locomotor ability in KA-treated *NLRP3*^{WT} and *NLRP3*$^{-/-}$ mice

(A) The movement time in the central area, (B) the movement time in the surrounding area, (C) the movement distance in the central area, and (D) the movement distance in the surrounding area. n = 10. Data are presented as mean ± S.E.M. ns, not statistically significant.

2.6 Effects of JC124 treatment on body weight and the histomorphology of major organs in mice

There were no significant differences in the body weights of the mice during the 4 weeks of JC124 or vehicle treatment (Supplementary Fig. 8A). Furthermore, treatment with JC124 did not affect the histomorphology of the major organs in mice, including the brain, liver, heart, lung, spleen, kidney, testis, and intestine (Supplementary Fig. 8B). These findings indicate that JC124 is safe for use in mice, which provides a promising foundation for future clinical trials and the potential transformation of JC124 into a clinically applicable treatment.

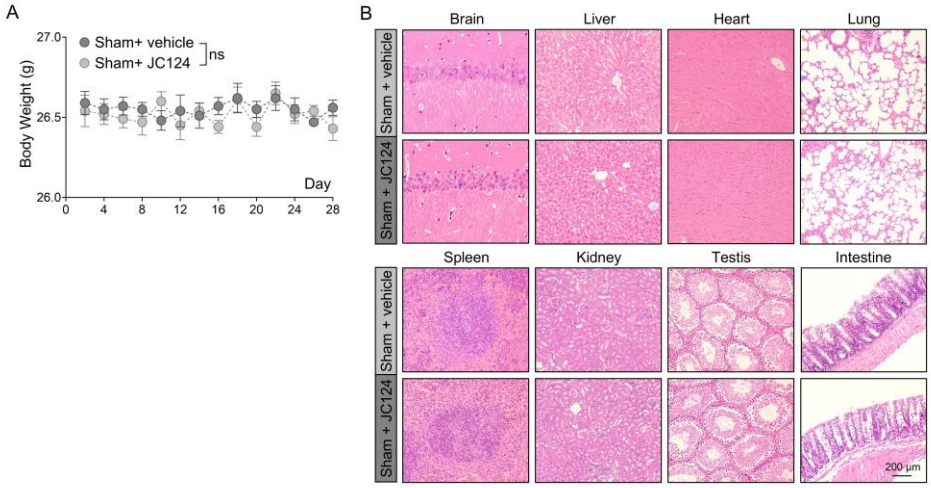

Supplementary Fig. 8 Effects of JC124 treatment on body weight and the histomorphology of major organs in mice

(A) Changes in the body weights of the mice during JC124 or vehicle treatment (n = 10). (B) Histological images of HE staining of the brain, liver, heart, lung, spleen, kidney, testis, and intestine of mice after JC124 or vehicle treatment (n = 6). Scale bar, 200 μm. Data represent the mean ± S.E.M. ns, not statistically significant.

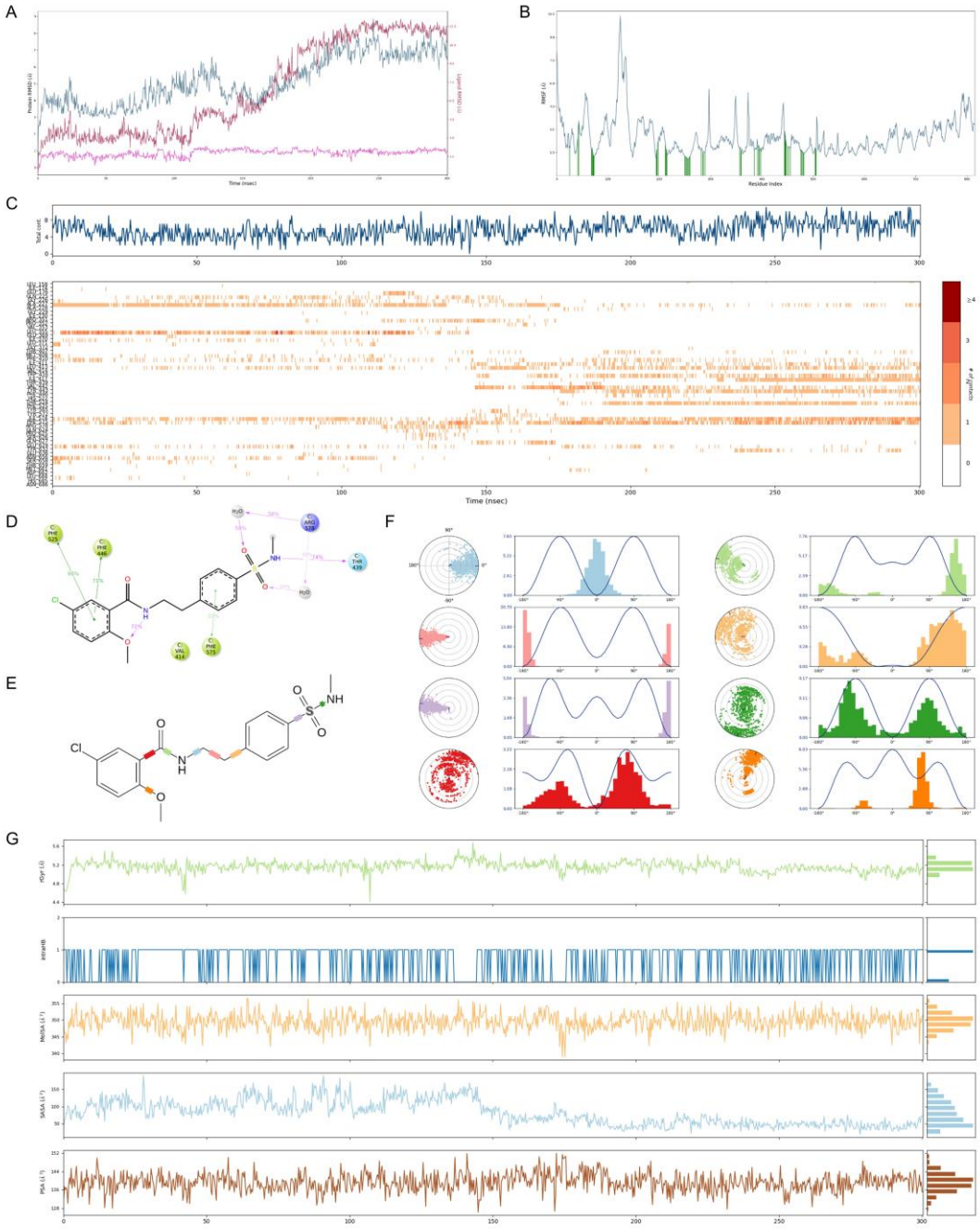

Supplementary Fig. 9 Molecular dynamics (MD) simulations of interactions between JC124 and the human NLRP3 protein

(A) Root mean square deviation (RMSD) for JC124 and the human NLRP3 protein. (B) Root mean square fluctuation (RMSF) for human NLRP3 protein. (C) Dynamic map of contacts between JC124 and the human NLRP3 protein residues over a duration of 300 ns. (D) Key residues involved in the binding of JC124 to the human NLRP3 protein. (E-F) Torsion angle radar plots of JC124. (G) Radius of gyration (rGyr), intramolecular hydrogen bonds (intraHB), molecular surface area (MolSA),

solvent accessible surface area (SASA), and polar surface area (PSA) of JC124.

References

1. Võsa U, Claringbould A, Westra HJ, et al. Large-scale cis- and trans-eQTL analyses identify thousands of genetic loci and polygenic scores that regulate blood gene expression. Nat Genet. 2021;53(9):1300-10.
2. Remi Stevelink CC, Siwei Chen BA, Oluyomi M Adesoji ZA, et al. GWAS meta-analysis of over 29,000 people with epilepsy identifies 26 risk loci and subtype-specific genetic architecture. Nat Genet. 2023;55(9):1471-82.
3. Yin J, Zhao F, Chojnacki JE, et al. NLRP3 Inflammasome Inhibitor Ameliorates Amyloid Pathology in a Mouse Model of Alzheimer's Disease. Mol Neurobiol. 2018;55(3):1977-87.
4. Kuwar R, Rolfe A, Di L, et al. A novel small molecular NLRP3 inflammasome inhibitor alleviates neuroinflammatory response following traumatic brain injury. J Neuroinflammation. 2019;16(1):81.
5. Sha L, Wang X, Li J, et al. Pharmacologic inhibition of Hsp90 to prevent GLT-1 degradation as an effective therapy for epilepsy. J Exp Med. 2017;214(2):547-63.
6. Sha L, Wu X, Yao Y, et al. Notch signaling activation promotes seizure activity in temporal lobe epilepsy. Mol Neurobiol. 2014;49(2):633-44.
7. Sha L, Chen T, Deng Y, et al. Hsp90 inhibitor HSP990 in very low dose upregulates EAAT2 and exerts potent antiepileptic activity. Theranostics. 2020;10(18):8415-29.
8. Yang Y, Tian X, Xu D, et al. GPR40 modulates epileptic seizure and NMDA receptor function. Sci Adv. 2018;4(10):2357.
9. Liu Y, Wang Y, Yang J, et al. G-alpha interacting protein interacting protein, C terminus 1 regulates epileptogenesis by increasing the expression of metabotropic glutamate receptor 7. CNS Neurosci Ther. 2022;28(1):126-38.
10. Zhang H, Tian X, Lu X, et al. TMEM25 modulates neuronal excitability and NMDA receptor subunit NR2B degradation. J Clin Invest. 2019;129(9):3864-76.
11. Sada N, Lee S, Katsu T, et al. Epilepsy treatment. Targeting LDH enzymes with a stiripentol analog to treat epilepsy. Science. 2015;347(6228):1362-7.

12. Zhang Z, Zhang H, Antonic-Baker A, et al. CXCR5 Regulates Neuronal Polarity Development and Migration in the Embryonic Stage via F-Actin Homeostasis and Results in Epilepsy-Related Behavior. Neurosci Bull. 2023;39(11):1605-22.

13. Qiao K, Xu C, Zhang C, et al. Discovery of an 8-oxoguanine regulator PCBP1 inhibitor by virtual screening and its synergistic effects with ROS-modulating agents in pancreatic cancer. Front Mol Biosci. 2024;11:1441550.

Original WB bands